

---

## Table of Contents: Supplementary Material

---

S1	Emission Datasets
S1.1	U.N. FAO-FRA 2015
S1.2	EDGARv4.3
S1.3	Houghton et al. (2012)
S1.4	Pan et al. (2011)
S1.5	DGVMs
S1.6	Tao et al. (2013)
S1.7	Achard et al. (2014)
S1.8	Harris et al. (2012)
S2	DGVM models, forcing datasets, and simulation protocols
S2.1	LULCC Dataset
S2.2	Climate and CO2 datasets
S2.3	DGVM models and Simulation setup
S3	Methods for Evaluating Biases in DGVM-modeled Carbon in Biomass
S4	Results for Trends in Forest Asia and Carbon in Biomass
S4.1	Changes in Forest Area
S4.2	Carbon in Biomass
S5	Literature Cited
S6	Tables
S7	Figures

---

## ***S1. Emissions Datasets***

### *S1.1 U.N. Food and Agriculture Organization 2015 Forest Resource Assessment*

The FAO-FRA 2015 defines natural forests as non-managed land with tree heights greater than 5 m, and a minimum canopy cover of 10 percent. Notably, this definition differs from those of MODIS-and-MERIS based remote-sensing studies, that require a minimum 60% canopy cover for the International Geosphere Biosphere program or 15% for the UN Land Cover Classification System (Poulter et al. 2011 GMD). Estimates of carbon stock-change in live biomass for different forest cover types are obtained through Tier 1 country-level reporting (IPCC Guidelines for National GHG Inventories 2006) and presented in the 2015 Forest Resource Assessment. Annual estimates of carbon stocks are obtained through linear interpolation from data in five-year reporting intervals. Land use emissions from deforestation, degradation or regrowth, are estimated by multiplying the carbon stock changes and the net area change in forest cover, whereas soil carbon flux and gross changes in land cover are not included for forested lands. The FAO-FRA also includes other land cover classes as a subset of agricultural lands, such as fallow land, permanent cropland, arable land, and temporary cropland. On agricultural lands, delayed or legacy, carbon emissions from the degradation of organic soils are included in the carbon emission estimates, but carbon emissions from product pools are not included. The soil carbon emissions are estimated as the area of managed land multiplied by climate-specific emissions factors reported in IPCC, 2006: Vol. 4, Ch. 5, Tab. 5.6. Data was downloaded via the FAO Statistics Division (FAOSTAT) website (<http://faostat.fao.org/>).

### *S1.2 Emission Database for Global Atmospheric Research*

EDGAR v4.3 (Petrescu et al. 2012) defines forest cover based on land cover delineations from the Global Land Cover (GLC 2000) map and the FAO Global Ecological Zone (GEZ) map to determine vegetation classes, and ultimately, the forest area. In EDGAR v4.3, the change in forest area was estimated by multiplying the fractional change in area from FAO-FRA reports, at the country level, and the forest area estimated by EDGAR v4.3 methodology at the country level. Emissions from deforestation were obtained by multiplying carbon stock emission factors per unit of area at the country-level, obtained from Tier 1 reporting (IPCC 2006), and the deforested area. Similar to the FAO-FRA approach, only emissions from net deforestation are estimated. However, EDGAR v4.3 also includes carbon emissions from fires (including fires from deforestation and forest degradation; natural fires in grasslands, savannas and forests; agricultural waste burning; and peat fires) using the Global Fire Emissions Database v3.1 (GFED) (van der Werf et al. 2010), which also includes carbon emissions from peat fires. A unique feature of the EDGAR v4.3 data is its inclusion of emissions from harvested wood products, obtained from FAO statistics on forest products production, import and export statistics. Emissions from wood harvest are instantaneous emissions and they reported as a separately in this study in order to make adequate comparison to estimates from other methods

that did not include this component emission. Forest regrowth was estimated using growth and yield equations summarized by dominant vegetation types with parameterization by eco-climate zones specific to each continent (Tier 1, IPCC 2006). For extended review of EDGAR v4.3, see Petrescu et al. (2012).

### *S1.3 Houghton et al. (2012)*

A bookkeeping model refined with more accurate data (Houghton 2010), which uses FAO-FRA statistics for present-day estimates of forest area and carbon stocks; annual statistics were obtained by interpolation between the 5-year FRA reporting schedule. The model estimates immediate carbon emissions from wood harvest and deforestation and long-term, legacy, carbon fluxes by tracking the per hectare carbon density in vegetation, soil and litter carbon pools. Average carbon stock per hectare was assigned based on ecosystem type (Houghton 2010). Forest regrowth was modeled, but it does not include the feedback of changes in climate or atmospheric CO<sub>2</sub> on biomass stocks. Carbon emissions from peat fires were not included in these estimates. Carbon emissions from wood harvest and shifting cultivation (gross land use changes), both of which increased the net LULCC emissions by 28% in the tropics compared to studies that did not include wood harvest or shifting cultivation (Houghton 2010).

### *S1.4 Pan et al. (2011)*

The LULCC emission estimates for Pan et al. (2011) were taken from the published article. In their study, separate methods were applied for calculating forest area, land use change, and carbon stock in regions corresponding to East Asia and Southeast Asia in this study. For China (East Asia, this study), Pan et al. determined forest area from country-level forest inventories using a forest definition of >20% canopy coverage. Carbon stock was determined using biomass expansion factors for each forest type in the inventory. Soil carbon to 1 m depth was estimated using a ratio of soil carbon to vegetated biomass. For Japan and Korea (East Asia, this study), forest area was estimated from systematic national forest inventories. Carbon stock was estimated from allometric relationships between above- and below-ground biomass and stem volume (biomass expansion factor), developed from the inventory data. For tropical Asia (Southeast Asia, this study), forest area was determined for intact forests, based on FAO-FRA reports and FRA forest definitions, whereas area of secondary forests were determined based on data from the Houghton et al. (2010) and Houghton (2012) bookkeeping model, which also incorporated FRA 2015 statistics. Carbon stock for tropical Asia was determined from the average carbon density estimate for tropical Africa and America because carbon stock data in tropical Asia were lacking at the time of their publication. Loss of soil carbon due to soil respiration (legacy flux) was not included. Changes in soil carbon stocks are not included in their emission estimates. Carbon emissions from wood harvest were included.

### *S1.5 Dynamic Global Vegetation Models*

Dynamic global vegetation models, or DGVMs, are ecosystem models that estimate growth and allocation of carbon using physiological representations. The DGVMs only required that land cover be distinguished to natural and managed fractions, with sub-tiles in each category corresponding to plant functional types, crop functional types or pasture. Above and belowground carbon stocks are thus a feature predicted by the model rather than prescribed parameters. The DGVM ensemble used prescribed land cover data directly or derived from the HYDE dataset (Goldewijk 2001) to simulate land cover change. The DGVM ensemble included 8 models from the ‘Trends in net land carbon exchange’ (TRENDY2) project, which varied in terms of PFTs, physiology, and demographic processes. Most models simulated net land use change, whereas CLMv4.5, LPX and VISIT models simulated gross changes in land use, i.e., the simultaneous clearing of forest for agriculture and abandonment of cropland in equal amounts. This means that models that simulated only net land use changes likely underestimate processes like shifting cultivation, which may result in no net loss of forest cover, but be associated with high land use emission fluxes (Houghton et al. 2012, Wilkenskjeld et al. 2014). Factorial model simulations were used to separate the effects of a time-varying climate and atmospheric CO<sub>2</sub> from emissions originating from LULCC. This DGVM simulation setup is equivalent to the “D3” uncoupled DGVM simulation detailed in Pongratz et al. (2014) and includes LULCC fluxes from net transitions, legacy fluxes, and loss of additional carbon sink capacity. The DGVM models simulated LULCC for years between 1901 and 2012; a detailed protocol of the simulation setup is provided by the Global Carbon Project TRENDY2 protocol (Sitch et al. 2015).

#### *S1.6 Tao et al. (2013)*

The LULCC emission estimates for Tao et al. (2013), taken from the published article, are provided as a comparison to the DGVM estimates analyzed in this study. In Tao et al. (2013), LULCC was defined by HYDE v3.1 (Goldewijk et al. 2011); only net land use changes were modeled. Carbon densities were estimated by a unique DGVM, the Dynamic Land Ecosystem Model (DLEM). DLEM also included effects on the carbon cycle from cropping system (e.g. non-wood harvest, rotation, fertilization and irrigation). Emissions from LULCC were estimated as the difference between simulations with- and without- land use change; the “D3” simulation setup in Pongratz et al. (2014).

#### *S1.7 Achard et al. (2014)*

The LULCC emission estimates for Achard et al. (2014) were taken from the published article. Tropical natural and managed forest cover were mapped at 3 ha spatial resolution using remote sensing surveys and automatic object-oriented classification on a combination of satellite imagery from TM Landsat 4,5 (1990) and ETM+ Landsat 7 (2000), as well as RapidEye, AVNIR-2, Kompsat, and Deimos-1 sensors imagery in 2010. Forest cover was defined as the summation between areas where canopy cover was greater than 70%, and one-half of the area where canopy

cover is 30-70%. Forest area change was determined as the difference in forest area delineations between satellite imagery in the reference year (1990, 2000) and 2010. Any deforestation or forest degradation occurring between 1990 and 2010, which may not have been captured in the imagery, would have been missed by the analysis. Carbon stock was determined using three independent data sources; these were Baccini et al. (2012), Saatchi et al. (2012), and the FAO Global Ecological Zone (GEZ) map combined with Tier 1 (IPCC 2006) carbon stock factors. Forest regrowth was determined as in EDGAR v4.3 (*section 2.1.2, above*).

### *S1.8 Harris et al. (2012)*

The LULCC emission estimates for Harris et al. (2012) were taken from the published article. Forest cover was mapped at 30 m resolution based on remote sensing surveys that applied stratified sampling of MODIS and Landsat ETM+ data. Carbon stock estimates were based on Saatchi et al. (2012) spatially-explicit biomass maps, which are based on GLAS lidar-derived tree heights combined with height-biomass allometric equations. Although Harris et al. (2012) describe their estimates as gross emissions they do not explicitly estimate emissions from shifting cultivation. Instead, the authors define their *gross* emissions as estimates that include committed (i.e. immediate) carbon emissions, while excluding forest regrowth and long-term carbon storage from wood products. Harris et al. (2012) do not include soil carbon fluxes (legacy flux).

## **S2. DGVM models, forcing datasets, and simulation protocols**

### *S2.1 Land Use and Land Cover Change (LULCC) Dataset*

LULCC was prescribed using the history database of the global environment (HYDE) dataset (Goldewijk 2001), which provides land use for both cropland and pasture as a fraction of a gridcell ( $0.5^\circ$ ) at an annual timestep from 1860 to 2012. The HYDE dataset is based on a statistical downscaling method that uses population as a proxy for agricultural activity, which was calibrated with modern data sources and hindcast for the historical period. Given the change in managed lands, DGVM modeling groups were responsible for determining rules for the land cover transitions (e.g. primary forest  $\rightarrow$  agriculture, or secondary forest  $\rightarrow$  agriculture, or grassland  $\rightarrow$  agriculture). One approach for estimating areal changes in forest is demonstrated in this study (Section SM4.1); this approach assumes an area-equivalent loss of forest for an increase in cropland or pasture. A few of the models (CLM4.5, LPX, VISIT) simulated gross land use transitions (i.e., from shifting cultivation), using wood harvest mass prescribed by the HYDE dataset. Additionally, CLMv4.5 and VISIT also included carbon fluxes from crop and wood harvesting, as well as irrigation and nitrogen fertilization of crops.

### *S2.2 Climate and CO<sub>2</sub> Datasets*

We used CRU or CRUNCEP reanalysis climate data (1901-2012) at a spatial resolution of 0.5 degrees. Global atmospheric CO<sub>2</sub> concentrations were prescribed at 287.14 ppm during the spin-up phase of the simulations (prior to year 1860), whereas annual (1860-2012) time-varying CO<sub>2</sub> data were obtained from ice core datasets and from the National Oceanic Atmospheric Administration and were used in transient simulations.

### *S2.3 Dynamic Global Vegetation Models and Simulation Setup*

LULCC emissions were estimated from an ensemble of Dynamic Global Vegetation Models (DGVM) that participated in the TRENDY2 model inter-comparison (Table S1). DGVMs were run for two land use change scenarios: a changing climate without LULCC (S2) and with LULCC (S3). The simulation setup is equivalent to the “D3” uncoupled DGVM simulation detailed in Pongratz et al. (2014). The factorial simulation allowed us to isolate emissions occurring from LULCC, independent of climate feedbacks. The carbon fluxes were obtained as Network Common Data Form (netcdf; Rew and Davis 1990) files and processed with the *ncdf* (Pierce 2011) and *raster* (Hijmans and van Etten 2012) package in R. The carbon emissions from LULCC were determined as the difference in Net Biome Production (NBP; defined as GPP – Rh – Fire Emissions, *sensu* Chapin III et al. 2006) between scenarios S3 and S2. Regional summaries in Asia were assessed using a regional mask provided by the Asia Pacific Network for Global Change Research. Graphical plots of the data were produced with the *ggplot2* (Wickham 2009) package in R.

The TRENDY2 Protocol required three simulation phases, (i) spin-up, (ii) transient 1860-1900, and (iii) transient 1901-2012. During spin-up, DGVMs were run to equilibrium using a constant CO<sub>2</sub> concentration of 287.14 ppm, a recycled 20-yr climate (preserving the mean and inter-annual variability) from the early decades of the 20<sup>th</sup> century (1901-1920), and a constant crop and pasture fractional distribution from the year 1860. The second phase (ii) of the simulation, transient 1860-1900, required that DGVMs continue to use the 20-yr recycled climate as in phase (i), and use time-varying CO<sub>2</sub> concentrations as prescribed by the data, and either a constant land use for scenario S2 or a time-varying LULCC for scenario S3, as prescribed by HYDE. In the final phase (iii) of the simulations, all DGVMs used time-varying CO<sub>2</sub> concentrations, time-varying climate data, and either a constant land use for scenario S2 or time-varying LULCC for scenario S3.

### ***S3.1 Methods for Evaluating Biases in DGVM-modeled Carbon in Biomass***

Baccini et al. (2012) estimated aboveground biomass of tropical forests using lidar returns of tree height from the GLAS sensor aboard the ICESAT satellite and relating the heights to allometric equations derived from ground-based measurements. The DGVMs simulated carbon stocks at the full extent of all regions in this study, whereas the Baccini et al. (2012) dataset only provided data in the tropics. Therefore, we clipped the geographic extent of the DGVM datasets to match the extent of the Baccini et al. (2012) data. For comparison between DGVM total carbon

in biomass and Baccini et al. (2012) aboveground biomass, we made a simplifying assumption for a ratio of 0.70 for aboveground biomass to total biomass, and also assumed that carbon was 50% of biomass; the JULES model assumed that carbon was 40% of biomass.

### ***S3.2 Methods for Cluster Analysis of Land Use Flux (LU flux) Estimates***

A cluster analysis was performed on LU flux estimates that were available for both the 1990s and 2000s (i.e., as a vector of estimates for 1990s and 2000s); all DGVM estimates were analyzed as separate estimates. A distance matrix was calculated on the LU flux vectors (Pg C), and the Euclidean distance between vectors was then used to determine unique clusters, regardless of the method (e.g., bookkeeping or DGVM).

## ***S4. Results for Trends in Forest Asia and Carbon in Biomass***

### ***S4.1 Changes in Forest Area***

In Southeast Asia during the 1990's, the FAO reported a decline in the forest area ( $-2.55 \text{ Mha yr}^{-1}$ ), which was higher than estimates by Achard et al. (2014) ( $-1.78 \text{ Mha yr}^{-1}$ ), Stibig et al. (2014) ( $-1.75 \text{ Mha yr}^{-1} \pm 0.26 \text{ S.E.}$ ), Kim et al. (2015) using Landsat data ( $-1.22 \text{ Mha yr}^{-1}$ ), and the HYDE data model ( $-0.73 \text{ Mha yr}^{-1}$ ). During the 2000s, the FAO-FRA reported a decline in forest area ( $-1.16 \text{ Mha yr}^{-1}$ ), which was of slightly lower magnitude than their estimates in the 1990's. A decreasing trend in forest loss, compared with individual estimates from 1990's, was also present in estimates by Achard et al. (2014) ( $-1.44 \text{ Mha yr}^{-1}$ ), and Stibig et al. (2014) remote sensing studies ( $-1.45 \text{ Mha yr}^{-1} \pm 0.25 \text{ S.E.}$ ). In contrast, Kim et al. (2015) reported increasing forest loss in the 2000s ( $-1.99 \text{ Mha yr}^{-1}$ ) compared to their 1990's estimate. The HYDE data model also suggested an increasing trend in forest loss during the 2000's ( $-1.28 \text{ Mha yr}^{-1}$ ). Even though the trend estimates differ among methods the magnitude of the estimates of forest loss are similar in the 2000's.

Published estimates, independent of FAO-FRA, on the magnitude of change in forest area for East and South Asia are scarce. In East Asia during the 1990's, the FAO-FRA reported an increase in forest area during the 1990's ( $+1.76 \text{ Mha yr}^{-1}$ ), whereas the HYDE data model suggested a decline in forest area during the 1990's ( $-0.45 \text{ Mha yr}^{-1}$ ). In the 2000's the FAO-FRA reported an increase in forest area ( $+2.70 \text{ Mha yr}^{-1}$ ), as did the HYDE data model ( $+0.91 \text{ Mha yr}^{-1}$ ). In South Asia during the 1990's, both the FAO-FRA ( $-0.0065 \text{ Mha yr}^{-1}$ ) and HYDE ( $-0.22 \text{ Mha yr}^{-1}$ ) reported a decrease in forest area. However, in South Asia during the 2000's, the FAO-FRA reported an increasing forest area ( $+0.21 \text{ Mha yr}^{-1}$ ) compared to their estimates from the 1990's, as did the HYDE data model ( $+0.24 \text{ Mha yr}^{-1}$ ).

### ***S4.2 Carbon in Biomass***

For all regions in this study, the total carbon in above and belowground live biomass, excluding litter and soil mineral carbon, reported by the FAO-FRA was 34.67 Pg C, whereas all DGVMs simulated higher total carbon in biomass, but individual DGVM estimates varied widely ([44.35, 121.63] Pg C). The wide range in estimates was driven largely by differences in simulated carbon in the Southeast Asia region (aboveground biomass in Figure S2). The standard deviation in total carbon in biomass across regions was largest in Southeast Asia ( $\pm 38.51$  Pg C), followed by East Asia ( $\pm 14.31$  Pg C), and lowest in South Asia ( $\pm 4.38$  Pg C). The DGVMs were in moderate agreement and suggested that 43-72% of total carbon in biomass from all regions came from Southeast Asia. Although the FAO-FRA reported much lower total carbon in biomass across all regions (Figure S2), the contribution of carbon in biomass from Southeast Asia (70% of total carbon in biomass) was consistent with the DGVMs.

The discrepancies among estimates from FAO-FRA statistics and individual DGVM models become more apparent when compared with the Baccini et al. (2012) and Liu et al. (2015) remote sensing estimates of carbon in aboveground live biomass (Figure S3). Baccini et al. (2012) and the Liu et al. (2015) estimates were in general agreement among the countries for which estimates were available in both studies. The FAO-FRA statistics were consistently below Baccini et al. (2012) and the difference ranged from 0.31 to 9.43 Pg C below Baccini et al. (2012) estimates, with the highest difference occurring in Indonesia (Figure S3). The CLMv4.5 and OCN models simulated carbon in aboveground live biomass that was consistently higher than the Baccini et al. (2012) benchmark (Figure S3). The CLMv4.5 model allocates an increasing fraction of NPP to woody biomass with increasing NPP in order to positively correlate the turnover of carbon in vegetation with productivity, but this results in an overestimated biomass in tropical forests (*see* Figure 4 in Negron-Juarez et al. 2015); the reason for the bias of OCN is unclear. The ORCHIDEE model lacked full coverage in insular Southeast Asia, and its estimates are therefore lowest among all the DGVMs. For Southeast Asia, when these three DGVMs were removed from the DGVM ensemble, the range in decadal mean land use flux (i.e., uncertainty in DGVM ensemble) is reduced by 38%, or 0.26 Pg C yr<sup>-1</sup> in the 1990's, and by 27%, or 0.14 Pg C yr<sup>-1</sup>, in the 2000's (Table S3). We thus exclude estimates made by CLMv4.5, OCN, and ORCHIDEE DGVMs in our reported emission estimates for the Southeast Asia region below.

Benchmark data for the other regions are lacking, and it is clear that FAO-FRA are an inadequate benchmark for determining DGVM bias (Figure S2). We made inferences from the country-level comparisons between Baccini et al. (2012) and Liu et al. (2015), which suggested good agreement among these independent studies (Figure S3). Therefore, the estimates for carbon in aboveground biomass from Liu et al. (2015) were used as a benchmark reference for the East and South Asia regions to justify omitting DGVM models that might be biased too high in their carbon stock estimates. We support the omission of the CLMv4.5, JULES, and OCN models from DGVM estimates in East Asia, because they corresponded to a difference of 14.2, 18.8, and 11.4 Pg C from the Liu et al. (2015) estimates, respectively. All DGVM



models were retained in the estimates for South Asia. Although the carbon emissions from the DGVMs vary widely, both within and among models (Figures S4-6), we feel that we successfully reduce and constrain our uncertainty in the emission estimate through the omission of biased models.

#### *S4.3 Cluster Analysis for LU flux estimates in 1990s and 2000s*

In Southeast Asia, most estimates suggested a general decline in emissions between decades, except for FAO-FRA. The FAO-FRA lacked a response in the regrowth sink to climate, which was present in the DGVMs, and it also utilized country-level carbon stock estimates, which together, resulted in higher LU fluxes than many DGVMs (Fig. S7). In Southeast Asia, higher LU fluxes from CLMv4.5 and OCN are due to a higher simulated biomass, whereas VISIT simulated biomass within range of the benchmark data, but it was singular in that it included fluxes from land management (Fig. S7). In East Asia, the Inventory and Bookkeeping methods lacked a response to climate and do not include legacy emissions; the latter is probably driving the larger LU flux estimate from the DGVMs (Fig. S8). In South Asia, the ORCHIDEE model, exhibited high inter-annual variability, suggesting a high-sensitivity to climate, which resulted in a higher overall LU flux estimate (Fig. S9). When comparing the OCN model to benchmark biomass data, it simulated higher biomass than other models, which probably drove the higher LU flux estimates in South Asia, as its estimate in other regions was also higher than other DGVMs. As in East Asia, VISIT was within range of the benchmark data for biomass, but it was unique in that it simulated carbon fluxes from wood harvest and land management.

#### **S5. Literature Cited**

1. Achard, F., R. Beuchle, P. Mayaux, H.-J. Stibig, C. Bodart, A. Brink, S. Carboni, B. Desclée, F. Donnay, H. D. Eva, A. Lupi, R. Raši, R. Seliger, and D. Simonetti. 2014. Determination of tropical deforestation rates and related carbon losses from 1990 to 2010. *Global Change Biology* 20:2540–54.
2. Baccini, A., S. J. Goetz, W. S. Walker, N. T. Laporte, M. Sun, D. Sulla-Menashe, J. Hackler, P. S. a. Beck, R. Dubayah, M. a. Friedl, S. Samanta, and R. a. Houghton. 2012. Estimated carbon dioxide emissions from tropical deforestation improved by carbon-density maps. *Nature Climate Change* 2:182–185.
3. Chapin, F. S., G. M. Woodwell, J. T. Randerson, E. B. Rastetter, G. M. Lovett, D. D. Baldocchi, D. A. Clark, M. E. Harmon, D. S. Schimel, R. Valentini, C. Wirth, J. D. Aber, J. J. Cole, M. L. Goulden, J. W. Harden, M. Heimann, R. W. Howarth, P. A. Matson, A. D. McGuire, J. M. Melillo, H. A. Mooney, J. C. Neff, R. A. Houghton, M. L. Pace, M. G. Ryan, S. W. Running, O. E. Sala, W. H. Schlesinger, and E. D. Schulze. 2006. Reconciling carbon-cycle concepts, terminology, and methods. *Ecosystems* 9:1041-1050.
4. Clark, D. B., L. M. Mercado, S. Sitch, C. D. Jones, N. Gedney, M. J. Best, M. Pryor, G. G. Rooney, R. L. H. Essery, E. Blyth, O. Boucher, R. J. Harding, C. Huntingford, and P. M. Cox. The Joint UK Land Environment Simulator

- (JULES), model description – Part 2: Carbon fluxes and vegetation dynamics. *Geosci. Model Dev.* 4:701–722, doi:10.5194/gmd-4-701-2011, 2011.
5. EDGAR. Emission Database for Global Atmospheric Research (EDGAR), release version 4.3. European Commission, Joint Research Centre (JRC)/Netherlands Environmental Assessment Agency (PBL): 2011. <http://edgar.jrc.ec.europa.eu>
  6. FAO-FRA 2015. Global Forest Resource Assessment 2015. Food and Agriculture Organization of the United Nations.
  7. Goldewijk, K. K. 2001. Estimating global land use change over the past 300 years: The HYDE Database. *Global Biogeochemical Cycles* 15:417–433.
  8. Goldewijk K. K., Beusen A, van Drecht G, de Vos M (2011) The HYDE 3.1 spatially explicit database of human induced land use change over the past 12,000 years. *Global Ecology and Biogeography* 20:73-86. doi:10.1111/j.1466-8238.2010.00587.x
  9. Hijmans, R. J., and J. van Etten. 2012. raster: Geographic analysis and modeling with raster data. R package version 2.0-12. <http://CRAN.R-project.org/package=raster>
  10. Houghton, R. A. 2010. How well do we know the flux of CO<sub>2</sub> from land-use change? *Tellus* 62B: 337-351.
  11. Houghton, R. A., J. I. House, J. Pongratz, G. R. Van Der Werf, R. S. Defries, M. C. Hansen, C. Le Quéré, and N. Ramankutty. 2012a. Carbon emissions from land use and land-cover change. *Biogeosciences* 9:5125–5142.
  12. Ito, A., M. Inatomi, W. Mo, M. Lee, H. Koizumi, N. Saigusa, S. Murayama, and S. Yamamoto. 2007. Examination of model-estimated ecosystem respiration by use of flux measurement data from a cool-temperate deciduous broad-leaved forest in central Japan. *Tellus B* 59:616–624.
  13. Krinner, G., N. Viovy, N. de Noblet-Ducoudré, J. Ogeé, J. Polcher, P. Friedlingstein, P. Ciais, S. Sitch, and I. C. Prentice. A dynamic global vegetation model for studies of the coupled atmosphere–biosphere system. *Global Biogeochem. Cy.* 19, GB1015, doi:10.1029/2003GB002199, 2005.
  14. Lawrence, D. M., K. W. Oleson, M. G. Flanner, P. E. Thornton, S. C. Swenson, P. J. Lawrence, X. Zeng, Z. L. Yang, S. Levis, K. Sakaguchi, G. B. Bonan, and A. G. Slater. Parameterization improvements and functional and structural advances in version 4 of the Community Land Model. *J. Adv. Model. Earth Syst.*, 3, M03001, doi:10.1029/2011MS000045, 2011
  15. Liu, Y. Y., A. I. J. M. van Dijk, R. A. M. de Jeu, J. G. Canadell, M. F. McCabe, J. P. Evans, and G. Wang. 2015. Recent reversal in loss of global terrestrial biomass. *Nature Clim. Change* 5:470–474.
  16. Negrón-Juárez, R. I., C. D. Koven, W. J. Riley, R. G. Knox, and J. Q. Chambers. 2015. Observed allocations of productivity and biomass, and turnover times in tropical forests are not accurately represented in CMIP5 Earth system models. *Environmental Research Letters* 10:064017. doi:10.1088/1748-9326/10/6/064017.
  17. Pan, Y., R. A. Birdsey, J. Fang, R. Houghton, P. E. Kauppi, W. A. Kurz, O. L. Phillips, A. Shvidenko, S. L. Lewis, J. G. Canadell, P. Ciais, R. B. Jackson, S. W.

- Pacala, A. D. McGuire, S. Piao, A. Rautiainen, S. Sitch, and D. Hayes. 2011. A large and persistent carbon sink in the world's forests. *Science* 333:988–993.
18. Petrescu, A. M. R., R. Abad-Vinas, G. Janssens-Maenhout, V. N. B. Blujdea, G. Grassi. 2012. Global estimates of carbon stock changes in living forest biomass: EDGARv4.3 – time series from 1990 to 2010. *Biogeosciences* 9:3437–3447.
  19. Pierce, D. 2011. ncd: Interface to Unidata netCDF data files, r package version 1.6.8.
  20. Pongratz, J., C. H. Reick, R. A. Houghton, and J. I. House. 2014. Terminology as a key uncertainty in net land use and land cover change carbon flux estimates. *Earth System Dynamics* 5:177–195.
  21. Poulter, B., P. Ciais, E. Hodson, H. Lischke, F. Maignan, S. Plummer, and N. E. Zimmermann. 2011. Plant functional type mapping for earth system models. *Geosciences Model Development* 4:993–1010.
  22. Prentice, I. C., D. I. Kelley, P. N. Foster, P. Friedlingstein, S. P. Harrison, and P. J. Bartlein. 2011. Modeling fire and the terrestrial carbon balance. *Global Biogeochem Cycles* 25:GB3005–GB3005.
  23. Rew, R., and G. Davis. 1990. NetCDF: An interface for scientific data access. *IEEE Computer Graphics and Applications* 10:76–82.
  24. Saatchi, S. S., N. L. Harris, S. Brown, M. Lefsky, E. T. A. Mitchard, W. Salas, B. R. Zutta, W. Buermann, S. L. Lewis, S. Hagen, S. Petrova, L. White, M. Silman, and A. Morel. 2011. Benchmark map of forest carbon stocks in tropical regions across three continents. *Proceedings of the National Academy of Sciences of the United States of America* 108:9899–9904.
  25. Sitch, S., B. Smith, I. C. Prentice, A. Arneth, A. Bondeau, W. Cramer, J. O. Kaplan, S. Levis, W. Lucht, M. T. Sykes, K. Thonicke, and S. Venevsky: Evaluation of ecosystem dynamics, plant geography and terrestrial carbon cycling in the LPJ dynamic global vegetation model. *Global Change Biology* 9:161–185, 2003.
  26. S. Sitch, P. Friedlingstein, N. Gruber, S. D. Jones, G. Murray-Tortarolo, A. Ahlström, S. C. Doney, H. Graven, C. Heinze, C. Huntingford, S. Levis, P. E. Levy, M. Lomas, B. Poulter, N. Viovy, S. Zaehle, N. Zeng, A. Arneth, G. Bonan, L. Bopp, J. G. Canadell, F. Chevallier, P. Ciais, R. Ellis, M. Gloor, P. Peylin, S. L. Piao, C. Le Quéré, B. Smith, Z. Zhu, and R. Myneni. 2015. Recent trends and drivers of regional sources and sinks of carbon dioxide. *Biogeosciences* 12:653–679.
  27. Smith, B., I. C. Prentice, and M. T. Sykes. 2001. Representation of vegetation dynamics in the modelling of terrestrial ecosystems: comparing two contrasting approaches within European climate space. *Global Ecology and Biogeography* 10:621–638.
  28. Tao, B., H. Tian, G. Chen, W. Ren, C. Lu, K.D. Alley, X. Xu, M. Liu, S. Pan, and H. Virji. 2013. Terrestrial carbon balance in tropical Asia: contribution from cropland expansion and land management. *Global and Planetary Change* 100:85–98. <http://dx.doi.org/10.1016/j.gloplacha.2012.09.006>.
  29. Van der Werf, G. R., J. T. Randerson, L. Giglio, G. J. Collatz, P. S. Kasibhatla, and A. F. Arellano. 2006. Interannual variability of global biomass burning

- emissions from 1997 to 2004. *Atmospheric Chemistry and Physics* 6:3423–3441.
30. Wickham, H. 2009. *ggplot2: elegant graphics for data analysis*. Springer, New York.
  31. Wilkenskeld, S., S. Kloster, J. Pongratz, T. Raddatz, and C. Reick. 2014. Comparing the influence of net and gross anthropogenic land use and land cover changes on the carbon cycle in the MPI-ESM. *Biogeosciences Discussions* 11:5443–5469.
  32. Zaehle, S., and A. D. Friend. 2010. Carbon and nitrogen cycle dynamics in the O-CN land surface model: 1. Model description, site-scale evaluation, and sensitivity to parameter estimates. *Global Biogeochemical Cycles* 24:GB1005. doi: 10.1029/2009GB003521

**S6. Tables**

**Table S1. Dynamic Global Vegetation Models (DGVM).**

DGVM	Abbreviation	Reference
Community Land Model	CLM 4.5	Lawrence et al. 2011
Joint UK Land Environment Simulator	JULES	Clark et al. 2011
Lund-Potsdam-Jena	LPJ	Sitch et al. 2003
Lund-Potsdam-Jena General Ecosystem	LPJ-GUESS	Smith et al. 2001
Land surface Processes and eXchanges	LPX	Prentice et al. 2011
Organising Carbon and Hydrology In Dynamic	ORCHIDEE	Krinner et al. 2005
Modified ORCHIDEE incld. a coupled carbon-	OCN	Zaehle, Friend 2010
Vegetation Integrative Simulator for Trace gases	VISIT	Ito et al. 2007

**Table S2. Countries by Regions used in this study.**

Region	Country
Southeast Asia	Brunei
	Cambodia
	Indonesia
	Laos
	Malaysia
	Myanmar
	Papua New Guinea
	Phillipines
	Singapore
	Thailand
Timor-Leste	
Vietnam	
East Asia	China
	Democratic People's Republic of Korea
	Japan
	Mongolia
	Republic of Korea
	Taiwan
South Asia	Bangladesh
	Bhutan
	India
	Nepal
	Pakistan

**Table S3. Decadal emission estimates from Land Use and Land Cover Change in Southeast Asia, obtained from an ensemble Dynamic Global Vegetation Models (DGVMs). The complete set in the DGVM ensemble is {CLM4.5, JULES, LPJ, LPX, OCN, ORCHIDEE, VISIT}. The ORCHIDEE model is omitted in both ensemble groupings below due to lack of coverage in insular Asia. An alternate ensemble grouping omits the CLM4.5 and OCN models from the estimates due to unreasonably high modeled biomass, as determined by evaluation against a remote-sensing-based biomass dataset (Baccini et al. (2012)).**

DGVM ensemble	Decade	N	Mean	S.D.	Max.	Min.
no ORCHIDEE	1980-1989	7	0.269	0.171	0.573	0.107
no ORCHIDEE, CLM4.5, OCN		5	0.194	0.112	0.390	0.107
no ORCHIDEE	1990-1999	7	0.376	0.218	0.734	0.127
no ORCHIDEE, CLM4.5, OCN		5	0.286	0.164	0.538	0.127
no ORCHIDEE	2000-2009	7	0.348	0.167	0.562	0.165
no ORCHIDEE, CLM4.5, OCN		5	0.283	0.149	0.532	0.165

## S7. Figures

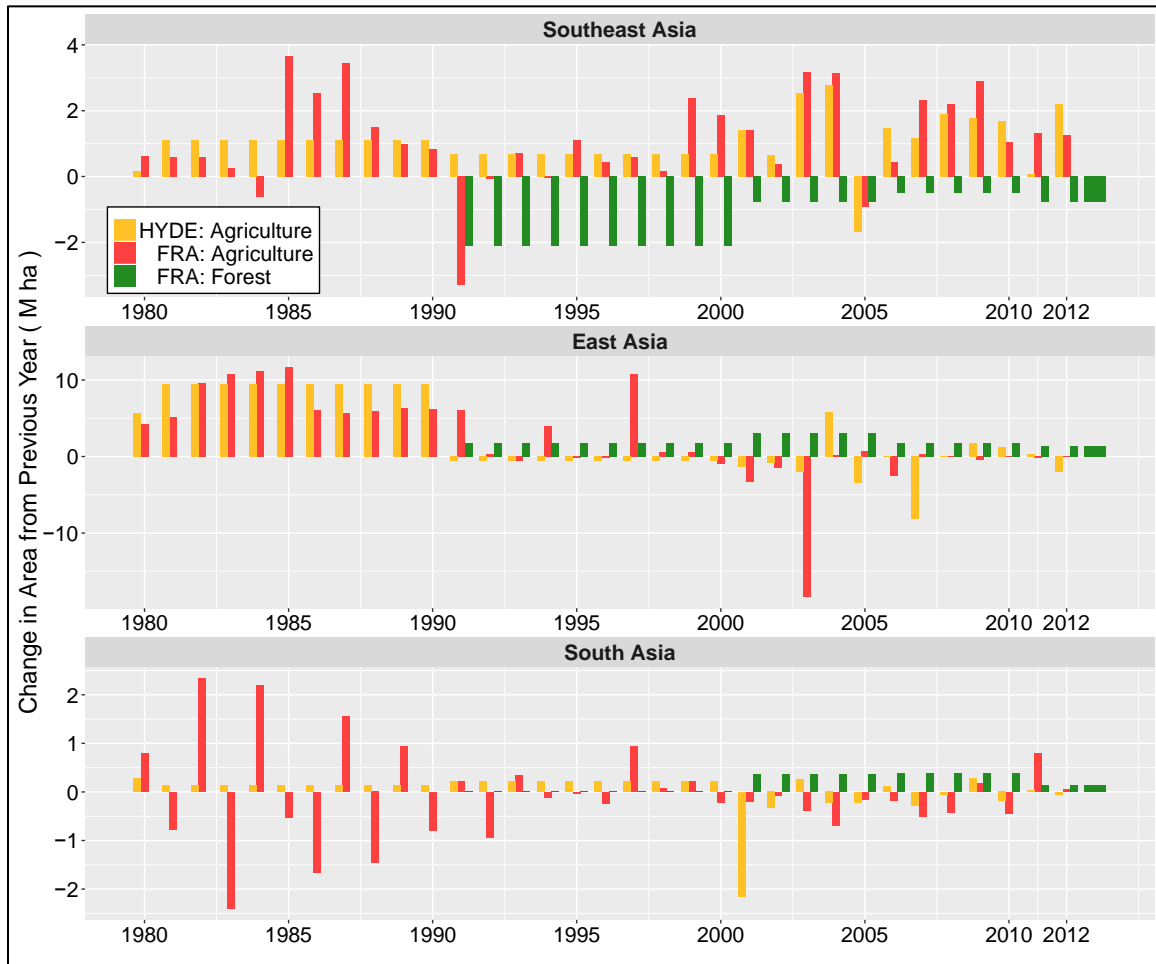


**Figure S1. Change in forest area and agricultural land as compared with the preceding year. The Forest Resource Assessment (FRA) 2015 reports {1990,1995,2000,2000} provide country-level statistics; annual estimates were obtained through linear interpolation between reporting years. The HYDE (Goldewijk 2001) database is used to prescribe land use change in the DGVM model simulations. The DGVM simulations assume that increases in agricultural land result in equivalent losses in forest area.**

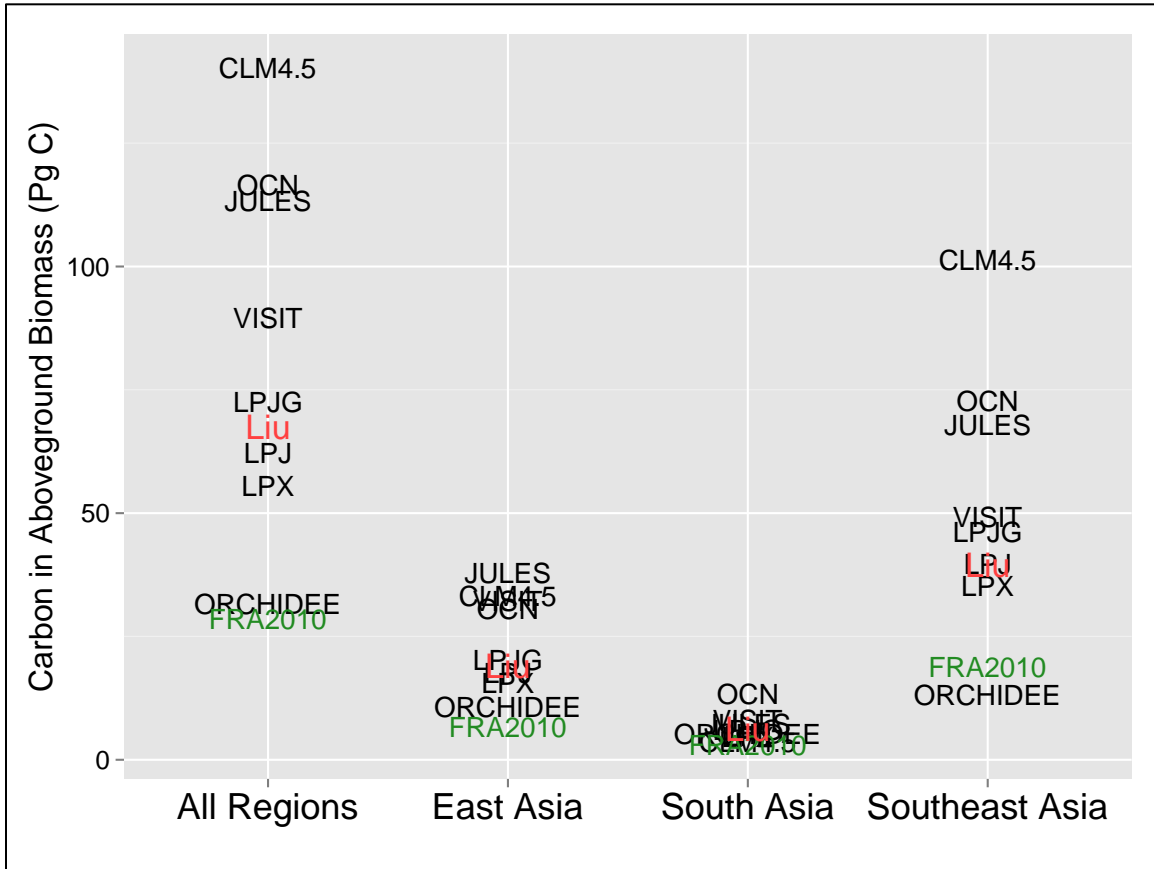
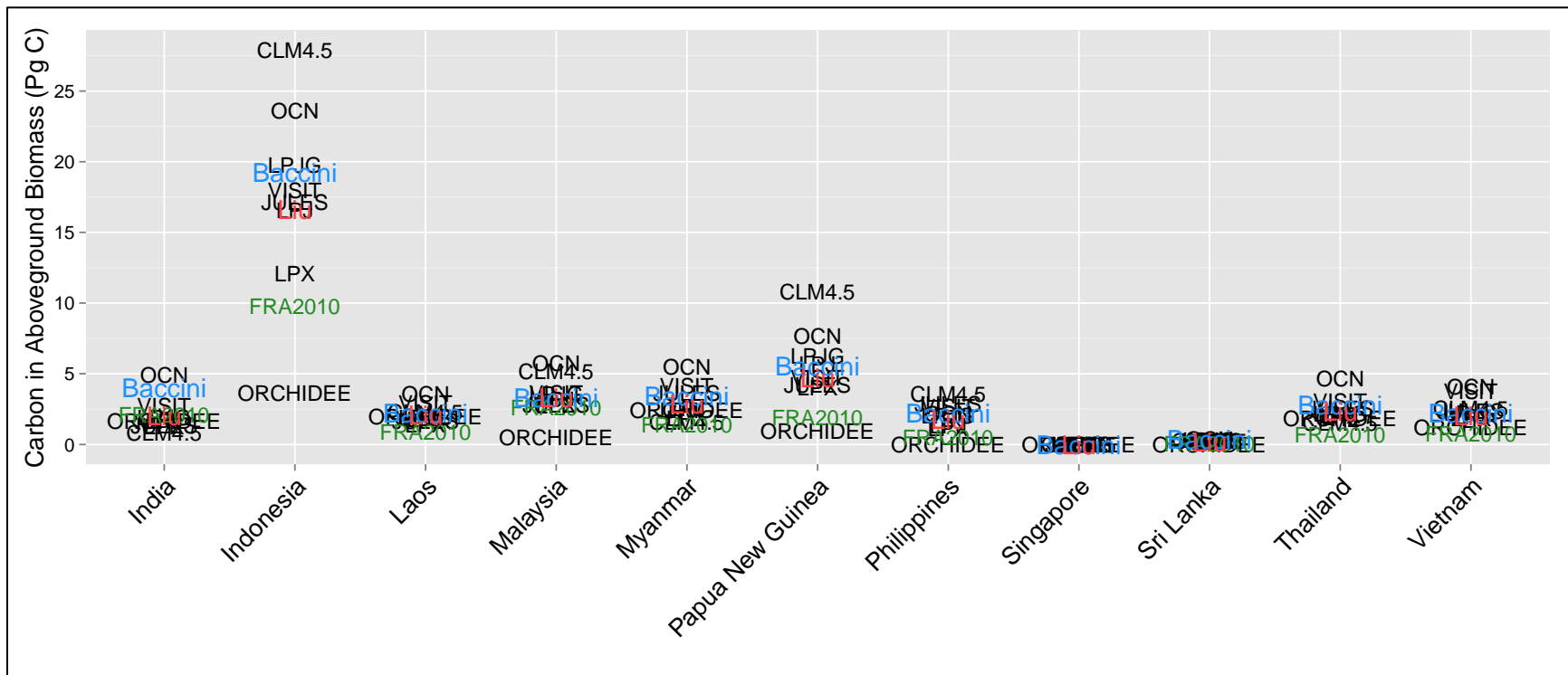


**Figure S2. Carbon in aboveground biomass estimated by the DGVMs (black text) for each geographic region in this study. The Forest Resource Assessment report in 2010 (FRA2010, green text) provides country-level biomass statistics using Tier 1 methods, but lack spatial heterogeneity. Regional estimates also presented from Liu et al. (2015) (red text), an independent remote-sensing study using microwave radiation from satellite observations.**



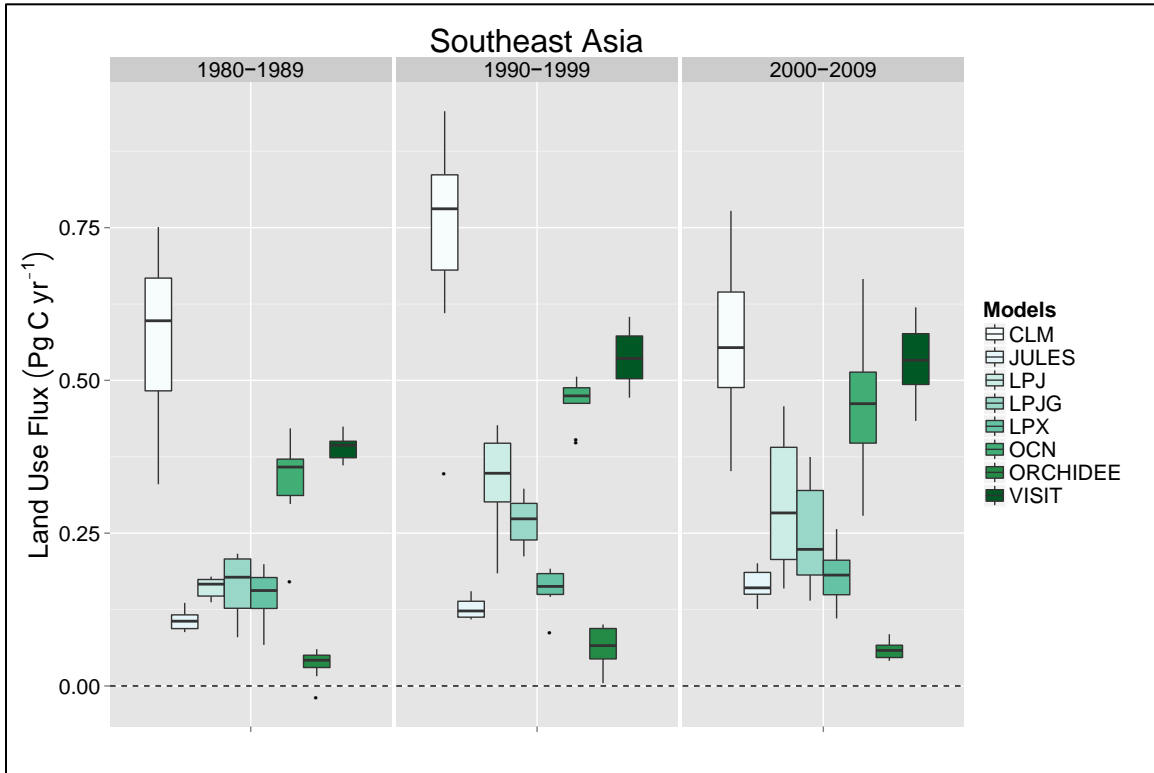




1

**Figure S3. Carbon in aboveground biomass for each country in the Baccini et al (2012) biomass dataset (blue text) that was within the geographic extent of this study; estimates from the DGVMs used in this study (black text), circa 2008 to match year of Baccini data; Tier 1 statistics from the Forest Resource Assessment 2010 report (FRA2010, green text); estimates also presented from Liu et al. (2015) (red text), an independent remote-sensing study using microwave radiation from satellite observations. DGVM datasets were clipped to match the extent of Baccini et al. (2012) data. FRA2010 data for Singapore are unavailable.**

2



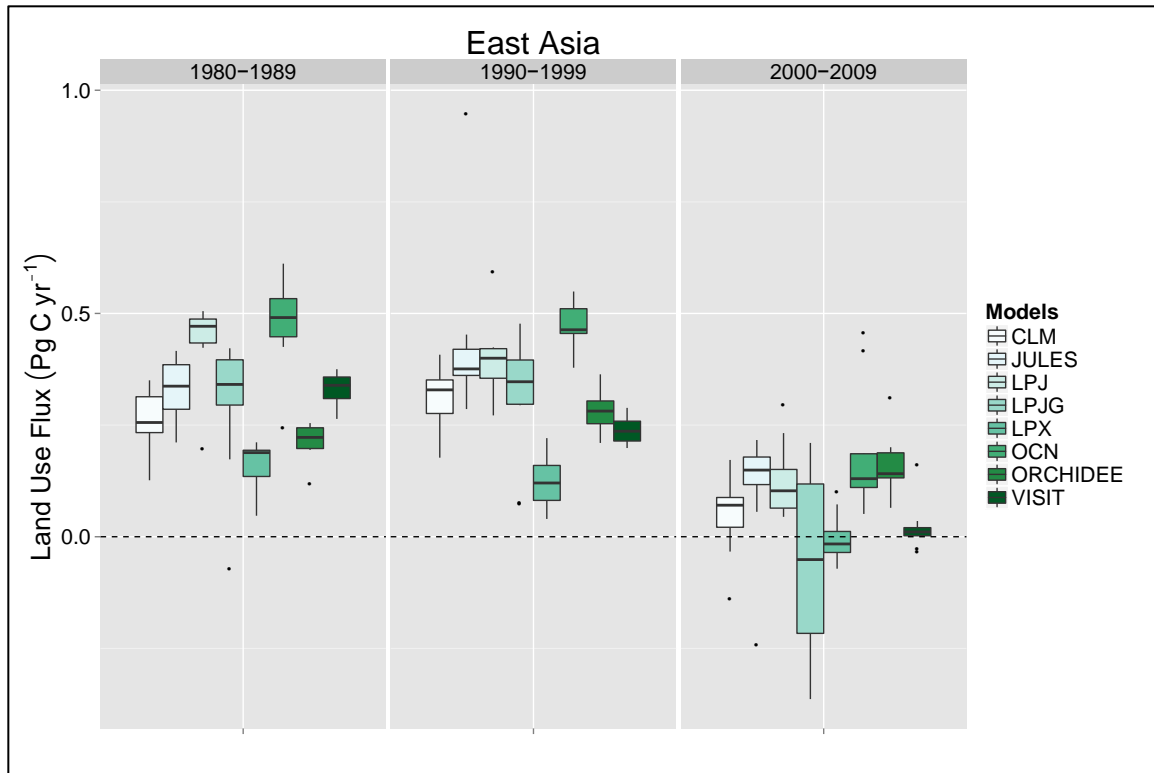
3

**Figure S4. Carbon emissions from LULCC (Land Use Flux) in Southeast Asia obtained the DGVM ensemble (boxplots are the interquartile range (inter-annual variability) with the median line, whiskers extend 1.5 times the IQ range). CLM is version 4.5. ORCHIDEE generally lacks of coverage over insular Asia. Individual DGVMs show the general increase in carbon emissions to the atmosphere after the 1980's, but few of the models show a decrease in LU fluxes from the 1990's to the 2000's.**

4

5

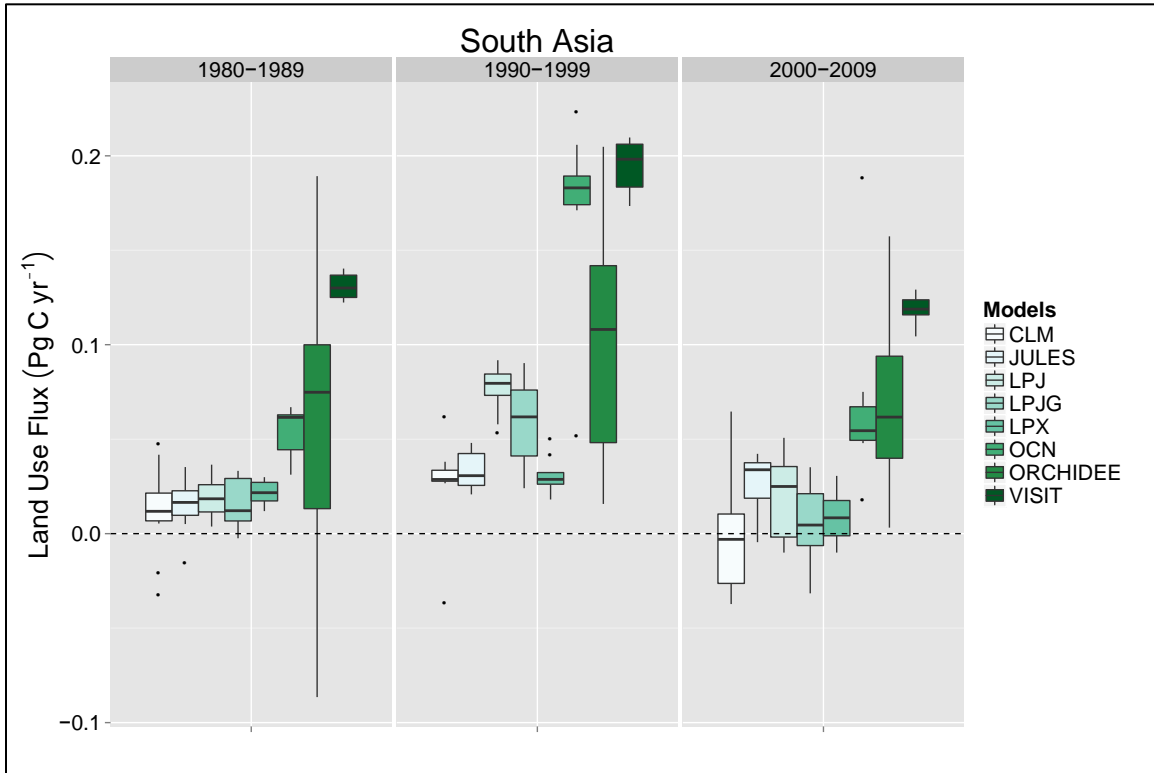
6



7  
8

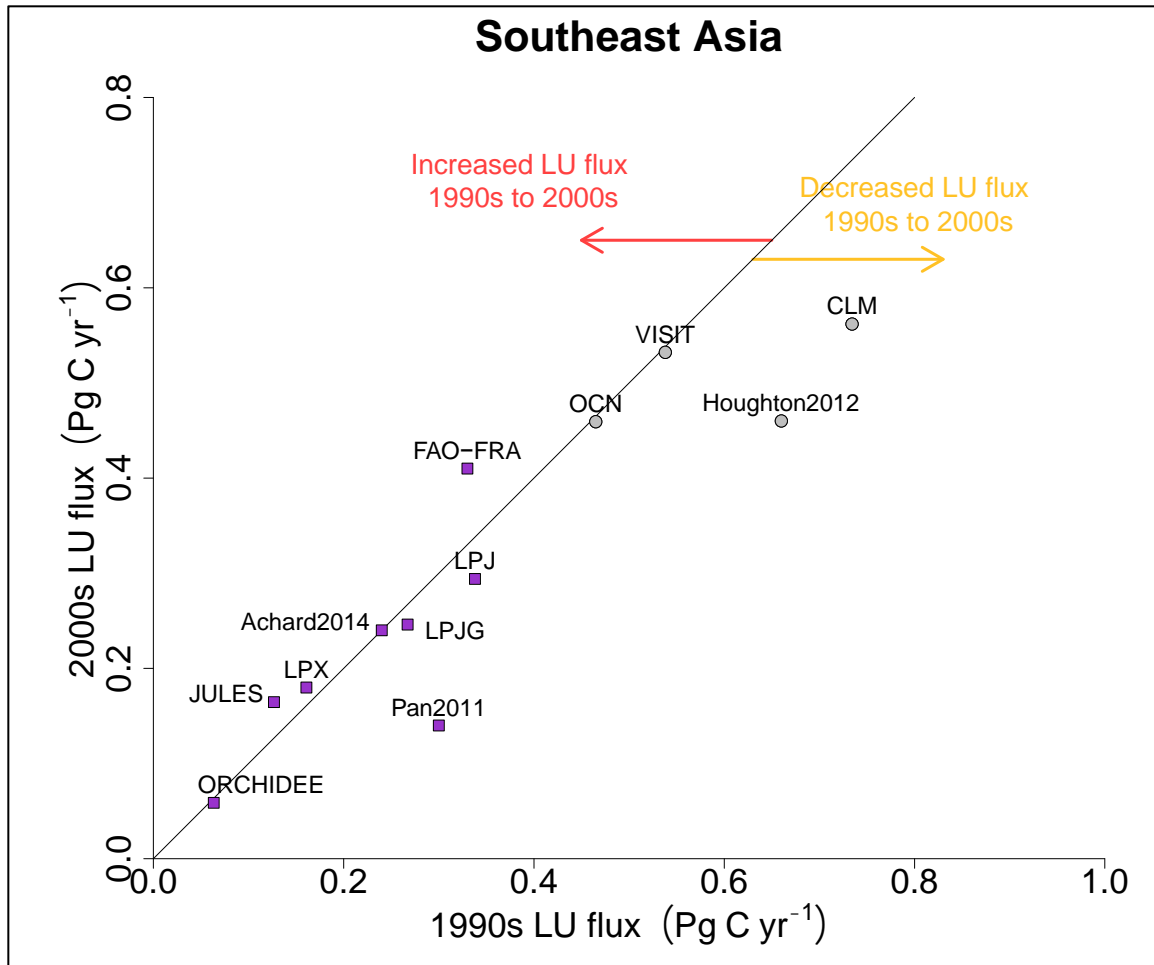
**Figure S5. Carbon emissions from LULCC (Land Use Flux) in East Asia obtained the DGVM ensemble (boxplots are the interquartile range (inter-annual variability) with the median line, whiskers extend 1.5 times the IQ range). CLM is version 4.5. The DGVMs show the general decline in carbon fluxes from the 1980's through the 2000's, which is mainly the result of extensive forest regrowth and afforestation efforts in the region. This decline in LU fluxes is also present in FAO statistics and EDGARv4.3 emissions statistics.**

9  
10

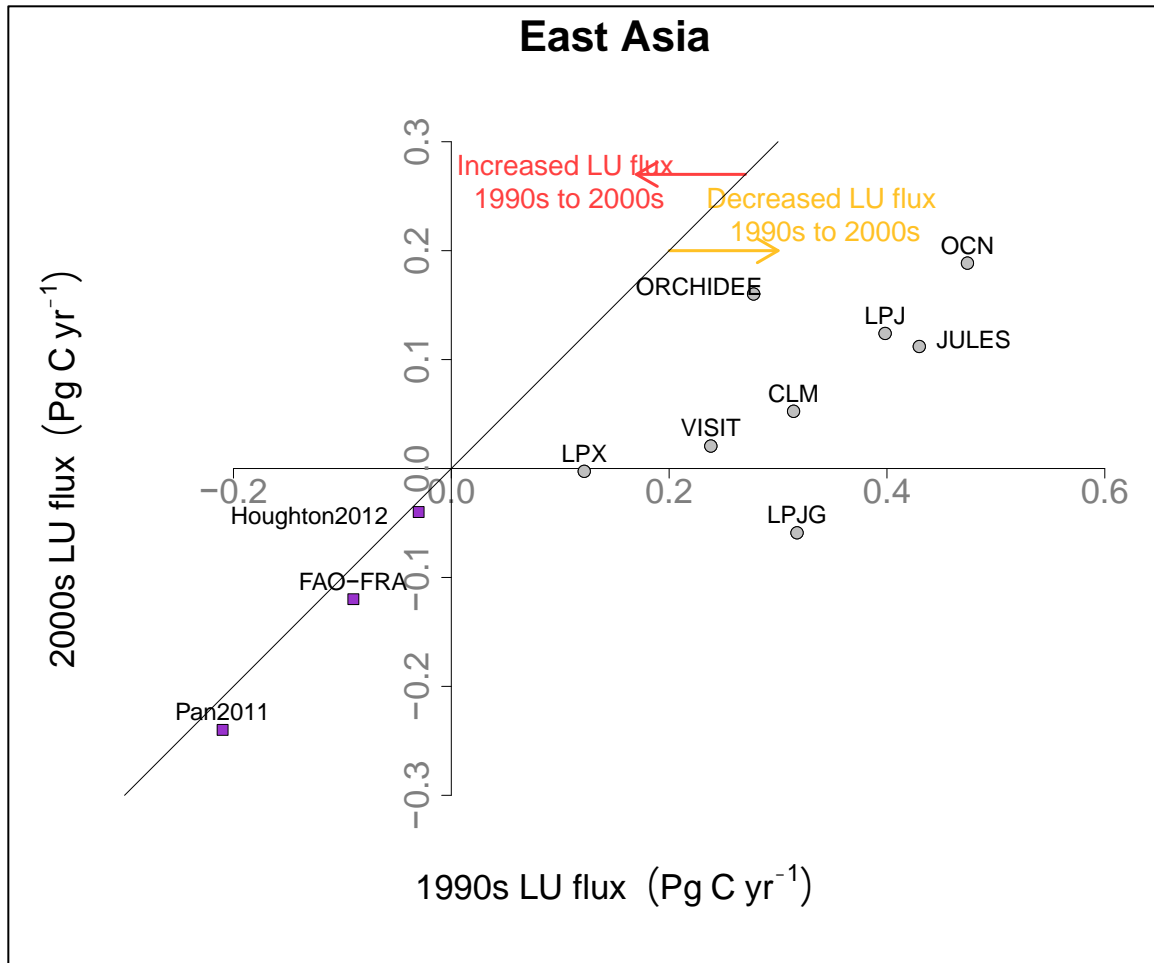


11  
 12  
 13  
 14  
 15  
 16  
 17  
 18  
 19  
 20

**Figure S6. Carbon emissions from LULCC (Land Use Flux) in South Asia obtained the DGVM ensemble (boxplots are the interquartile range (inter-annual variability) with the median line, whiskers extend 1.5 times the IQ range). CLM is version 4.5. The OCN, ORCHIDEE, and VISIT DGVMs estimate high fluxes in South Asia, but the driving mechanisms are unclear.**

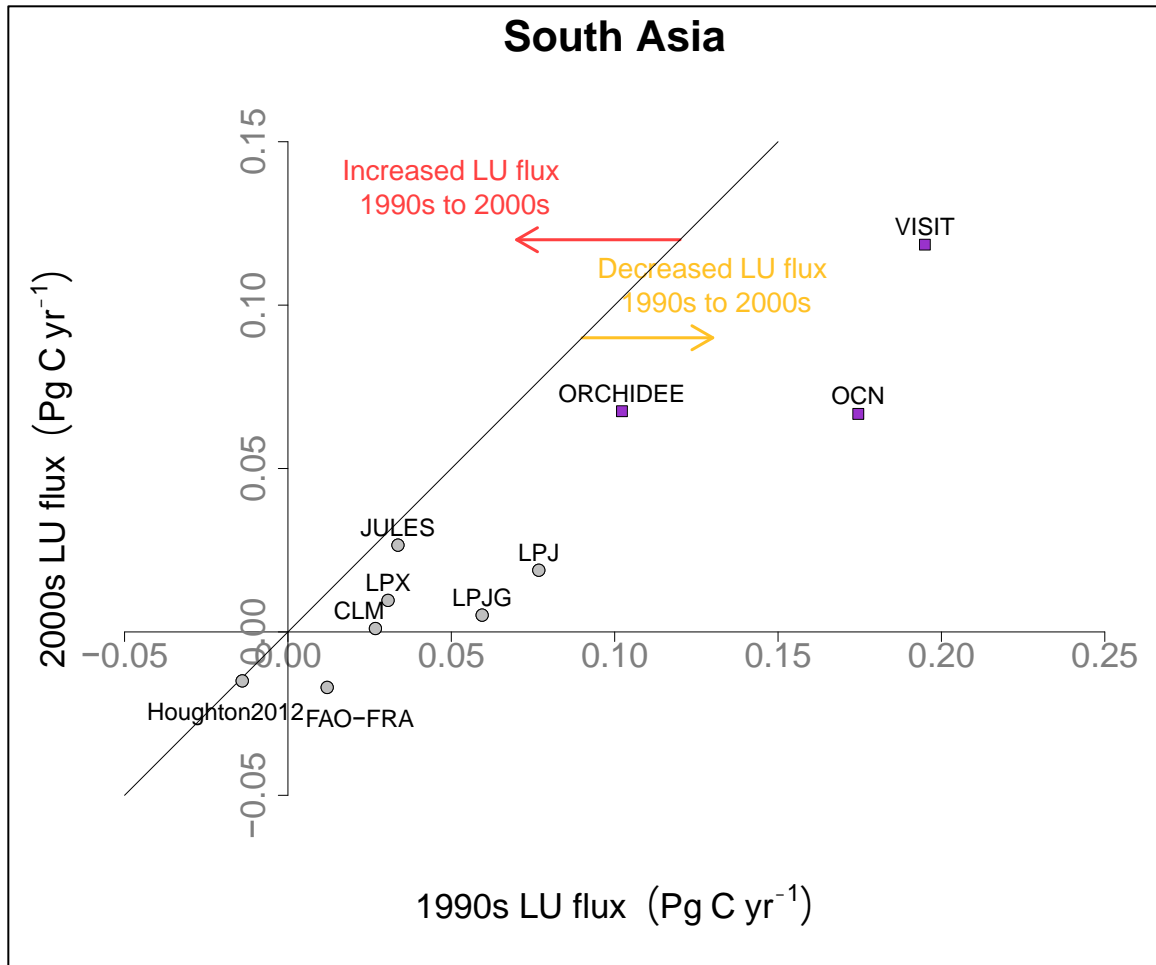


21  
 22 **Figure S7. Land use fluxes (LU flux) in 1990s versus 2000s for Southeast Asia,**  
 23 **for all 8 DGVMs (CLM is version 4.5), FAO-FRA (2015), the bookkeeping model**  
 24 **(Houghton2012), Achard et al. 2014 (Achard2014) and Pan et al. 2011**  
 25 **(Pan2011). The symbol and color groups represent distinct groupings from a**  
 26 **clustering algorithm based on the average Euclidean distance of the LU fluxes**  
 27 **in each estimate for both decades. The diagonal (1:1) line represents LU fluxes**  
 28 **that are similar between decades.**  
 29



30  
31  
32  
33  
34  
35

**Figure S8. Land use fluxes (LU flux) in 1990s versus 2000s for East Asia, for all 8 DGVMs (CLM is version 4.5.), FAO-FRA (2015), the bookkeeping model (Houghton2012), and Pan et al. 2011 (Pan2011). See Figure S7 legend for additional details.**



36  
37  
38  
39  
40

**Figure S9. Land use fluxes (LU flux) in 1990s versus 2000s for South Asia, for all 8 DGVMs (CLM is version 4.5), FAO-FRA (2015), the bookkeeping model (Houghton2012). See Figure S7 legend for additional details.**